Mechanism of the OH-Initiated Oxidation of Glycolaldehyde over the Temperature Range 233−296 K

Nadezhda I. Butkovskaya,* Nicolas Pouvesle, Alexandre Kukui,† and Georges Le Bras

CNRS, Laboratoire de Combustion et Systèmes Réactifs, 1C Av. de la Recherche Scientifique, 45071 Orléans Cedex 2, France

Received: August 3, 2006; In Final Form: October 3, 2006

The mechanism of the gas-phase OH-initiated oxidation of glycolaldehyde ($HOCH_2CHO$) was studied in the 233−296 K temperature range using a turbulent flow reactor coupled with a chemical ionization mass spectrometer. In the presence of O_2, formaldehyde, CO_2, formic acid, and glyoxal were observed at room temperature with the yields of 80, 34, 18, and 14%, respectively. Decrease of temperature to 233 K led to significant changes in the yields of the stable products: those of formaldehyde and glyoxal decreased to 50 and 4%, respectively, whereas that of formic acid increased to 52%. It was also found that the OH + glycolaldehyde + O_2 reaction proceeds with considerable reformation of OH radicals (by 25% at 296 K). The observed product yields are explained by a mechanism including formation of short-lived intermediate adducts of the primary radicals with O_2. The implication of the obtained results for the HO_x budget in the upper troposphere is discussed.

1. Introduction

Glycolaldehyde (GLAL, $HOCH_2CHO$) is produced in the atmosphere from the oxidation of several volatile organic compounds (VOCs) including ethene, 2-methyl-3-buten-2-ol (MBO), and isoprene.[1−3] GLAL is a major secondary generation product of the OH-initiated oxidation of isoprene.[4] GLAL can be also directly emitted into the atmosphere from biomass burning.[5] This hydroxyaldehyde has been detected in the lower troposphere at the ppb level [e.g., 6]. It can also be present in the upper troposphere (UT) where it can be transported from the surface by fast convection. It can also be produced in the UT from convectively transported precursors. In particular, convectively transported isoprene has been suggested as a potential source of HO_x (OH, HO_2) in the UT,[7,8] which influences the ozone budget. The assessment of the HO_x formation potential of isoprene and other GLAL precursors in the UT requires knowledge of the detailed mechanism of the oxidation of these compounds, in particular, the kinetics and mechanism of the title reaction at the low temperatures of the UT. The major removal process of GLAL in the atmosphere appears to be OH reaction and photolysis.[9,10] Rate constant and branching ratio of the OH reaction at ambient temperature were determined in three studies.[1,9,10] A recent study of this reaction using a pulsed laser photolysis−laser-induced fluorescence method gave a rate constant practically independent of temperature in the range of 240−362 K.[11]

Reaction of OH with glycolaldehyde can proceed through three abstraction channels:

$$OH + HOCH_2CHO \rightarrow HOCH_2CO + H_2O \quad (1a)$$

$$\rightarrow HOCHCHO + H_2O \quad (1b)$$

$$\rightarrow OCH_2CHO + H_2O \quad (1c)$$

The branching ratio of channels 1a and 1b $k_{1a}:k_{1b} \approx 80:20$ was obtained by Niki at al. in their FTIR chamber study in air in the presence of NO, whereas channel 1c was considered as negligible.[1] This branching ratio was confirmed in the study of Magneron et al. using a Teflon bag and the EUPHORE chamber with FTIR analysis of the species.[10] However, the mechanism of the oxidation was not completely understood. In both works, CH_2O, CO_2, and glyoxal ($(CHO)_2$) were observed as major products. The former two products were explained by reactions of the $HOCH_2C(O)OO$ adduct:

$$HOCH_2CO + O_2\ (+M) \rightarrow HOCH_2C(O)OO \quad (2)$$

$$HOCH_2C(O)OO + NO \rightarrow CH_2OH + CO_2 + NO_2 \quad (3)$$

$$2HOCH_2C(O)OO \rightarrow 2CH_2OH + 2CO_2 + O_2 \quad (4)$$

$$CH_2OH + O_2 \rightarrow CH_2O + HO_2 \quad (5)$$

Formation of glyoxal was attributed to eq 6 which follows channel 1b:

$$HOCHCHO + O_2 \rightarrow (HCO)_2 + HO_2 \quad (6)$$

In addition, CO was detected by Magneron et al. among the reaction products with a yield comparable to that of CH_2O. Niki et al. observed CO formation in the reaction of GLAL with Cl-atoms in air, following a mechanism similar to that with OH but with less selective abstraction ($k_a:k_b = 65:35$).[1] It was suggested that CO is formed in the secondary reactions of formaldehyde and glyoxal as follows:

* Author to whom correspondence should be addressed. E-mail: bout@cnrs-orleans.fr. Permanent address: Institute of Chemical Physics of the Russian Academy of Sciences, Moscow, Russian Federation.

† CNRS, Service d'Aéronomie, Paris.

10.1021/jp064993k CCC: $33.50
Published on Web 11/30/2006

$$CH_2O + OH\ (Cl) \rightarrow HCO + H_2O\ (HCl) \quad (7)$$

$$(HCO)_2 + OH\ (Cl) \rightarrow HCO + CO + H_2O\ (HCl) \quad (8)$$

$$HCO + O_2 \rightarrow CO + HO_2 \quad (9)$$

Also, formic acid, HCOOH, was detected in the Cl + GLAL system.[1] The pathway leading to HCOOH formation remained uncertain. The ultimate products of the vinoxy oxide from the minor channel (1c) in the presence of O_2 are CH_2O, CO, and HO_2 either through a prompt dissociation reaction (10) followed by reaction (9) or reaction with O_2 reaction (11):

$$OCH_2CHO \rightarrow CH_2O + HCO \quad (10)$$

$$HCO + O_2 \rightarrow CO + HO_2 \quad (9)$$

$$OCH_2CHO + O_2 \rightarrow CH_2O + CO + HO_2 \quad (11)$$

In our recent study of the OH-initiated oxidation of hydroxyacetone ($CH_3C(O)CH_2OH$), we have shown that the oxidation mechanism changes with temperature.[12] The study revealed that the peroxy radical formed via addition of O_2 to the major primary radical, $CH_3C(O)CHOH$, can rapidly decompose to give unexpected formic and acetic acids products. Extending the mechanism suggested to explain the formation of these acids in the oxidation of hydroxyacetone to the present study, one can expect formation of formic acid from the oxidation of glycolaldehyde.

The aim of the present work was to determine a detailed mechanism of reaction (1) over the 233−296 K temperature range by direct detection of reaction products in the presence of molecular oxygen. The experimental technique was a turbulent flow reactor combined with a chemical ionization mass spectrometer. The experiments were carried out at low initial OH concentrations to make negligible secondary radical−radical reactions within a residence time in the reactor less than 30 ms. As most of the final products were the same as in the OH + hydroxyacetone + O_2 system, the detection, calibration, and data treatment methods were similar to those previously described.[12]

2. Experimental Section

Chemical reactions took place in the turbulent flow reactor (TFR) coupled with the chemical ionization mass spectrometer (CIMS) (Figure 1). A flow of N_2 carrier gas in the TFR corresponded to the Reynolds number Re ≈ 7300 at a pressure of 200 Torr and typical flow velocity of 18 m s^{-1}. A detailed description of the experimental setup and a validation of flow and mixing conditions was reported in previous works from this laboratory.[12−14]

OH radicals were produced either in F + H_2O → OH + HF or in H + NO_2 → OH + NO reactions occurring in a movable injector. H- and F-atoms were generated by a microwave discharge in H_2/He or F_2/He gas mixtures. To study reactions with F-atoms, F_2/He mixture was used without introduction of H_2O in the injector. F-atom concentrations were determined by chemical titration using their fast reaction with methanol. Tank-grade H_2 and F_2 (Alpha Gaz 2) were used without further purification. OD radicals were generated by the D + NO_2 → OD + NO reaction using discharge in D_2/He gas mixture. NO_2 was prepared by keeping a mixture of NO with O_2 during 24 h followed by pumping out the oxygen through a liquid N_2 trap. Then, NO_2 diluted in He (1% and 12% mixtures) was stored in glass flasks. The OH radical signal was calibrated by the consumption of NO_2 in the H + NO_2 → OH + NO reaction when low concentrations of NO_2 were introduced into the main reactor as described previously.[14] Typical OH concentrations were (1−4) × 10^{11} molecule cm^{-3}. The maximum distance from the injector tip to the orifice of the inlet cone of the ionization zone was 50 cm, which corresponded to the reaction time in the TFR of about 30 ms.

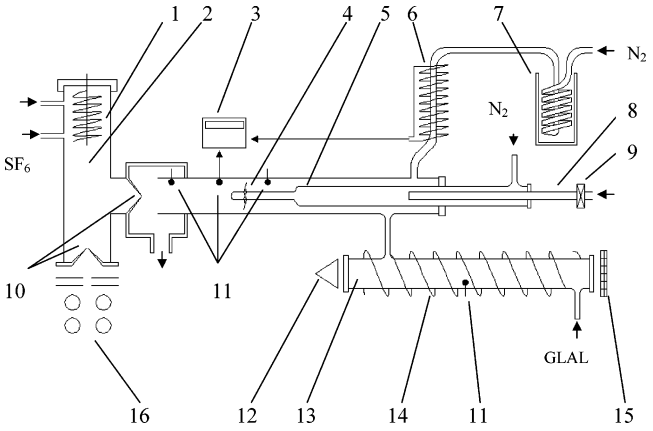

Figure 1. Experimental setup: 1, ion source; 2, ion molecule reactor; 3, temperature controller; 4, ≪turbulizer≫; 5, injector; 6, resistance; 7, cooling bath; 8, discharge tube; 9, microwave discharge; 10, sampling cones; 11, temperature sensor; 12, UV lamp; 13, absorption cell; 14, resistance; 15, UV detector.

Glycolaldehyde (GLAL) was introduced into the reactor upstream of the tip of the movable injector along with He flow passing through the trap containing GLAL. GLAL powder (Aldrich, crystalline) was heated to 60−62 °C. The inlet line including absorption cell (1-m long) was heated to 40 °C. Concentration of GLAL was measured online by UV absorption at λ = 254 nm (Hg lamp). The absorption spectroscopic measurements of GLAL concentrations were verified using chemical titration by known concentrations of F-atoms. The CIMS signal intensity of GLAL as a function of concentration was linear in the (1−40) × 10^{12} molecule cm^{-3} range. The following compounds were used for calibration purposes: formic acid (Riedel−deHaën, 98−100%), methanol (Riedel−deHaën, 99.9%), and CO_2 (Alpha Gaz N45). Their flow rates were measured by the change of pressure in a calibrated volume using pre-prepared mixtures in He.

A gas mixture from the TFR entered the ion−molecule reactor (IMR) through an orifice in a Teflon cone. The flow velocity of Ar carrier gas in the IMR was 20 m s^{-1} at 0.7 Torr pressure. The primary Ar^+ ions and free electrons were generated in the ion source by a heated filament. SF_6 was continuously introduced into the IMR downstream from the ion source. The primary SF_6^- (and a few percent of fragment F^-) negative ions were produced by attachment of thermalized electrons to SF_6. OH radicals and NO_2 were detected as OH^- (*m*/*e* 17) and NO_2^- (*m*/*e* 46) ions formed by electron transfer from SF_6^-.[15] HO_2 radicals were detected at *m*/*e* 140 as $SF_4 \cdot O_2^-$ ion formed in reaction with SF_6^-.[16] CO_2 molecules were detected, as in our previous work,[12] by CO_3^- ions (*m*/*e* 60), produced by the reaction

$$O_3^- + CO_2 \rightarrow CO_3^- + O_2$$

the O_3^- ions being obtained by charge transfer after adding ozone to the SF_6 flow. GLAL, CH_2O, $(HCO)_2$, HCOOH, and CH_3OH were detected using proton-transfer reactions (PTR) with $H_3O^+ \cdot (H_2O)_n$ (n = 0−3) ions produced by addition of H_2O into the IMR. Organic products with proton affinity (PA) higher

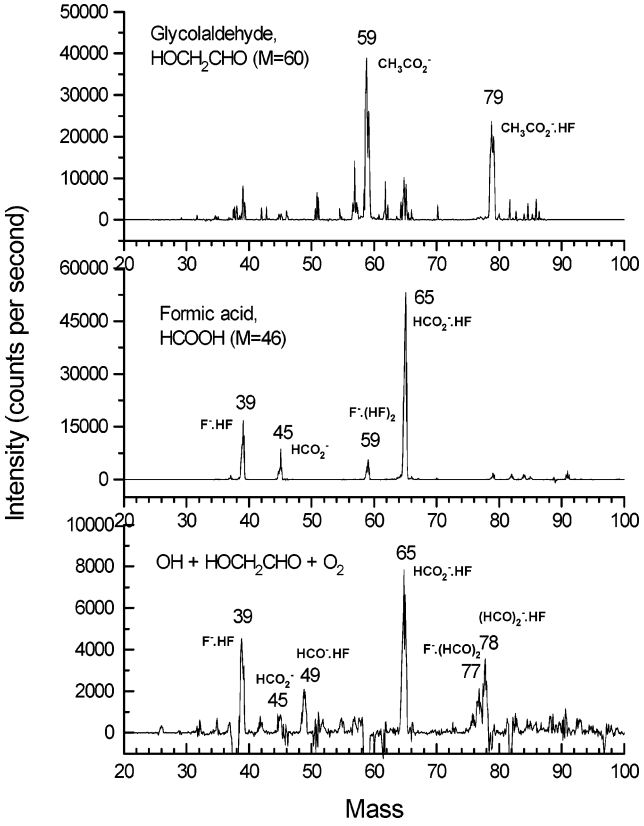

Figure 2. Negative spectra of glycolaldehyde (top), formic acid (center), and products from the $HOCH_2CHO + OH + O_2$ chemical system (bottom).

than that of H_2O (165 kcal mol^{-1}) can be detected as MH^+ and its water cluster ions by proton transfer:

$$H_3O^+\cdot(H_2O)_n + M \rightarrow MH^+\cdot(H_2O)_m + (H_2O)_{n-m+1}\ (n \geq m)$$

Accordingly, CH_2O (PA = 170.4 kcal mol^{-1}) was detected at *m*/*e* 31 and 49, $(HCO)_2$ (PA = 167 kcal mol^{-1}) at *m*/*e* 59, CH_3-OH (PA = 180.3 kcal mol^{-1}) at *m*/*e* 33 and 51, HCOOH (PA = 170.4 kcal mol^{-1}) at *m*/*e* 47 and 65, and GLAL (PA = 187 kcal mol^{-1}) at *m*/*e* 61 and 79.

Detection of organic compounds in negative mode was also used to identify reaction products as well as to provide a simultaneous control of the reactant during the measurements of OH and HO_2 kinetics. A negative spectrum of GLAL (Figure 2, top panel) consists of two main lines at *m*/*e* 59 and 79, which were, respectively, assigned to $CH_3CO_2^-$ and $CH_3CO_2^-\cdot HF$ ions produced presumably in the reactions with SF_6^-:

$$HOCH_2CHO + SF_6^- \rightarrow CH_3CO_2^- + SF_5 + HF$$
$$\rightarrow CH_3CO_2^-\cdot HF + SF_5$$

Negative spectra helped to identify formic acid among the reaction products. Figure 2 shows a negative spectrum of formic acid and a negative spectrum of the reaction products in the $OH + GLAL + O_2$ system. The peaks at *m*/*e* 45 and 65 in the spectrum of HCOOH correspond to the $COOH^-$ and $COOH^-\cdot HF$ ions produced in the reactions with SF_6^- similarly to GLAL. The lighter ion can also be formed in the reaction with F^-, which is considerably more exothermic than the reaction with SF_6^-:

$$HCOOH + F^- \rightarrow COOH^- + HF$$

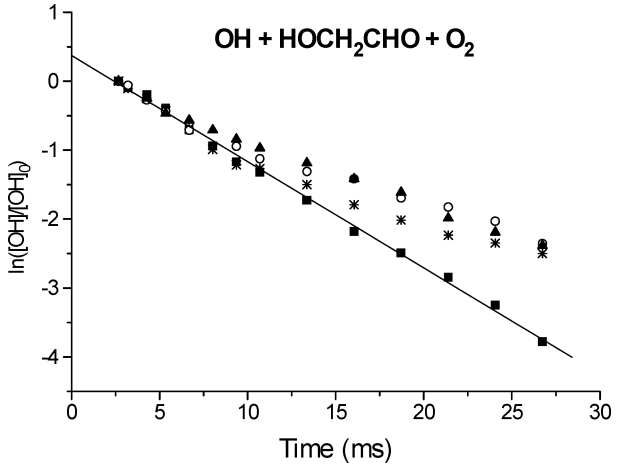

Figure 3. Temporal OH decay profiles in the OH + GLAL reaction with oxygen filter (■), at background O_2 concentration (*), and with added oxygen $[O_2] = 3 \times 10^{14}$ (○) and 1×10^{15} (▲) molecule cm^{-3}.

The peaks at *m*/*e* 39 and 59 can be assigned to $F^-\cdot HF$ and $F^-\cdot(HF)_2$ ion clusters. The product spectrum presents a difference between the discharge on and discharge off measurements. In addition to the formic acid peaks, it contains a peak at *m*/*e* 49 (presumably $HCO^-\cdot HF$ ion) and an *m*/*e* 76, 77, 78 triad, that could origin from ion−molecule reactions of glyoxal.

3. Results and Discussion

3.1. OH Reformation. Kinetics of the OH consumption in excess of GLAL was measured at different O_2 concentrations. Faster decays of the OH signal intensity were observed when a Cu-catalyst filter removing oxygen from the main N_2 flow in the TFR was used. This filter decreased the background O_2 concentration (usually about 1×10^{13} molecule cm^{-3}) by approximately a factor of 5. Also, a nonlinear dependence of ln([OH]) on reaction time was found at background O_2 concentration without the filter (Figure 3). Such behavior indicates a significant OH reformation in the presence of molecular oxygen.

To determine the fraction of the reformed OH concentration, β, we use a method consisting in the comparison of the kinetics of the OH and OD radicals in the GLAL + O_2 chemical system:

$$OH + HOCH_2CHO + O_2 \rightarrow \text{products other than OH } (1\text{-}\beta)$$
$$\rightarrow OH + \text{products } \beta$$
$$OD + HOCH_2CHO + O_2 \rightarrow \text{products other than OH } (1\text{-}\beta)$$
$$\rightarrow OH + \text{products } \beta$$

The corresponding kinetic equations were derived in our recent work.[12] This method needs to determine a value of the kinetic isotope effect (KIE), that is, the ratio of the rate constants of the OH and OD reactions with GLAL, $KIE = k_{OH}/k_{OD} = k_1/k_{1D}$:

$$OH + HOCH_2CHO \rightarrow \text{products} \quad (1)$$

$$OD + HOCH_2CHO \rightarrow \text{products} \quad (1D)$$

The rate constants k_1 and k_{1D} were measured under the pseudo-first-order conditions with respect to OH and OD, using $[OH] \approx [OD] \approx 2 \times 10^{11}$ molecule cm^{-3} and $[GLAL] > 2 \times 10^{12}$ molecule cm^{-3}. Figure 4a and 4b presents an example of the measurements of ln([OD]) and ln([OH]) versus reaction time

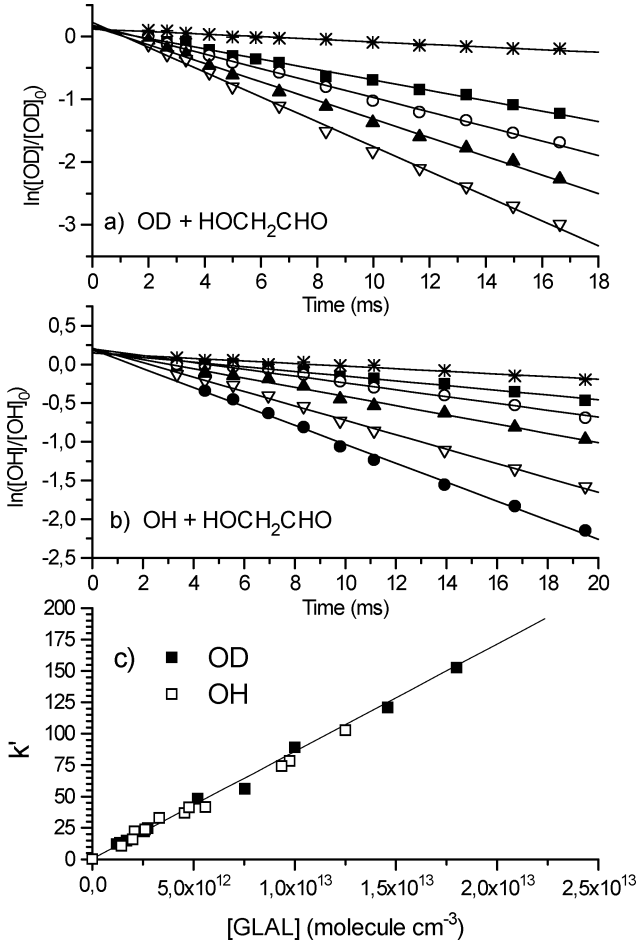

Figure 4. Measurements of k_1 and k_{1D}: (a) first-order OD decay at [GLAL] = 0 (*), 7.5×10^{12} (■), 1.0×10^{13} (○), 1.45×10^{13} (▲), and 1.8×10^{13} (▽) molecule cm^{-3}; (b) first-order OH decay at [GLAL] = 0 (*), 2.5×10^{12} (■), 4.5×10^{12} (○), 6.0×10^{12} (▲), 9.8×10^{12} (▽), and 1.25×10^{13} (●) molecule cm^{-3}; (c) dependence of the pseudo-first-order rate constants on GLAL concentration.

at different GLAL concentrations. To prevent the OH reformation, the latter was measured using the oxygen filter. The measured pseudo-first-order rate constants for both reactions as a function of GLAL concentration are presented in Figure 4c. The obtained rate constants are $k_1 = (8.2 \pm 0.4) \times 10^{-12}$ and $k_{1D} = (8.5 \pm 0.2) \times 10^{-12}$ cm^3 molecule^{-1} s^{-1}. The difference between the two values is within the error limits (2σ) showing a negligible secondary KIE for the OH/OD reaction with GLAL. The k_1 value is in excellent agreement with the absolute value from the study of Karunanandan et al.,[11] $(8.0 \pm 0.8) \times 10^{-12}$ cm^3 molecule^{-1} s^{-1}, though it is less than the values obtained in relative measurements: $(1.0 \pm 0.2) \times 10^{-11}$ of Niki et al.,[1] $(1.1 \pm 0.3) \times 10^{-11}$ of Bacher et al.,[9] and $(1.2 \pm 0.3) \times 10^{-11}$ cm^3 molecule^{-1} s^{-1} of Magneron et al.[10]

When $k_1 = k_{1D}$, the fraction of reformed OH is given by a simple expression,

$$\beta = \frac{p_2 - p_1}{p_2 - k_{loss}}$$

where p_1 is the slope of the plot of ln{[OH]/[OH]$_0$} versus reaction time, p_2 is the slope of ln([OD]/[OD]$_0$) versus reaction time, and k_{loss} is the first-order rate constant of the OH and OD losses in the absence of GLAL. This definition of p_1 corresponds to separate introduction of OH and OD into the reactor. In case of simultaneous introduction, p_1 denotes the slope of the temporal plot of ln{([OH] + [OD])/([OH]$_0$ + [OD]$_0$)}. In this scheme, β represents all the possible pathways of the secondary OH formation reactions and not only reactions of the primary radicals with O_2. Such processes could be, for example, reactions of HO_2 with the primary radicals or NO:

TABLE 1: Measurements of the OH Reformation Yield in the OH/OD + Glycolaldehyde + O_2 System[a]

T (K)	k_{loss}	p_1	p_2	Φ(OH)
295	18 ± 1	78.97	98.7	24.5
		83.4	104.7	24.5
296	25 ± 1	74.2	92.3	26.9
273	18 ± 1	78.5	102.3	32.6
253	18 ± 1	76.1	109.4	36.4
233	25 ± 1	61.9	90.7	43.8

[a] k_{loss} is the rate constant of the OH and OD losses in the absence of GLAL; p_1 and p_2 are the slopes of the plots of ln([OH] + [OD]) and ln([OD]) vs reaction time, respectively. See text for calculation of Φ(OH).

$$HO_2 + HOCH_2CO \rightarrow CH_2OH + CO_2 + OH \quad (12)$$

$$HO_2 + HOCHCHO \rightarrow (HCO)_2 + 2OH \quad (13)$$

$$HO_2 + NO \rightarrow OH + NO_2 \quad (14)$$

However, because of low initial OH and OD concentrations, such reactions were unimportant, and β could be identified as the fraction of OH reformation in reactions of primary radicals with O_2, Φ(OH). Table 1 reports the results of two experiments where OH and OD kinetics were simultaneously measured at different temperatures in the range 233−295 K. The decay profiles from the first experiment at $T = 295$, 273, and 253 K are shown in Figure 5. The data at $T = 295$ K were acquired before cooling the reactor and after cooling and restoration of room temperature. The initial concentrations were [GLAL] = 1.0×10^{13}, [O_2] = 1.2×10^{15}, [OH] = 2.1×10^{11}, and [OD] = 4.5×10^{11} molecule cm^{-3}. The rate constants of the hydroxyl radical losses in the absence of the reactant were 17.6 ± 0.9 s^{-1} and 18.4 ± 0.8 s^{-1} for OH and OD, respectively, and included self-reaction, reactions with NO_2 and NO, and wall loss. Another experiment was carried out at $T = 296$ and 233 K with approximately the same initial concentrations of the reactants. This experiment confirmed the measured reformation yield of OH at $T = 295$ K and its noticeable increase with lowering temperature (up to 44% at 233 K).

Although we did not carry out a special measurement to determine temperature dependence of the rate constant, our results obtained for different temperatures at fixed GLAL concentration confirm a weak (if any) change of k_1 with temperature in the 233−295 K range (see ref 11).

3.2. Product Yields. *CH_2O, $(HCO)_2$, and HCOOH.* The yields of formaldehyde, glyoxal, and formic acid at different temperatures were measured in the PTR regime by monitoring their mass-spectral peaks *m*/*e* 31 and 49, *m*/*e* 59, and *m*/*e* 47, respectively. Reactant concentrations were [GLAL] = 4.8×10^{12} and [O_2] = 1.2×10^{15} molecule cm^{-3}. OH radicals were produced in F + H_2O reaction. The product yield was determined as Φ(product) = Δ[product]/Δ[GLAL] at reaction time $t = 27$ ms. GLAL consumption was measured by the change of the intensity of the peak at *m*/*e* 61, and it practically did not change with temperature. The average Δ[GLAL] = $(1.98 \pm 0.09) \times 10^{11}$ molecule cm^{-3} was taken for the calculation of the product yields. The CH_2O signal was calibrated as previously in ref 12, producing CH_2O by the reaction of F-atoms with CH_3OH in the presence of high O_2 concentration (~5×10^{16}

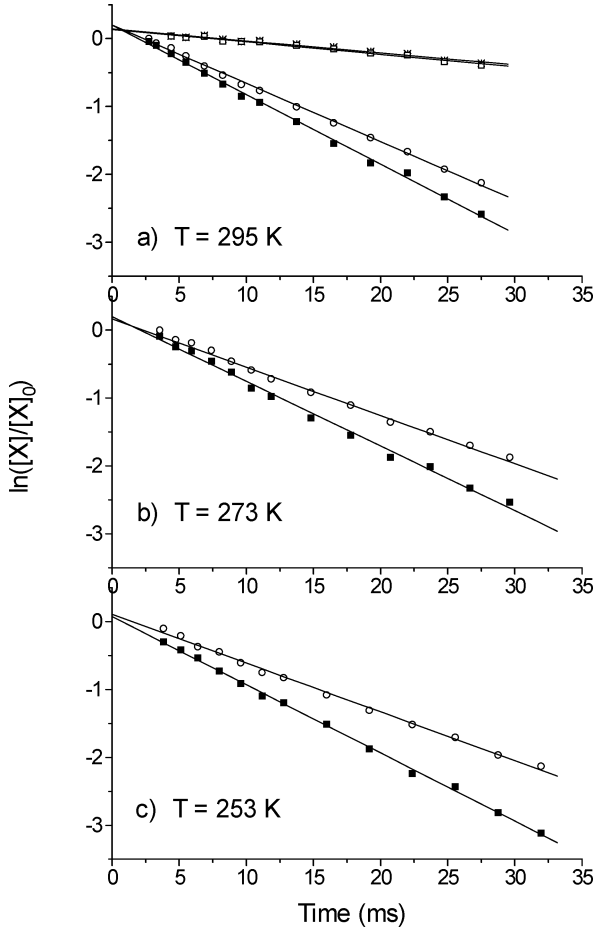

Figure 5. Temporal dependence of ln[OD] (■) and ln([OH] + [OD]) (○) at three temperatures and [GLAL] = 1×10^{13} and [O_2] = 1.2×10^{15} molecule cm^{-3}. Upper plot in top panel is ln[OD] (□) and ln[OH] (*) in the absence of GLAL.

molecule cm^{-3}). HCOOH was calibrated by introducing a known flow of diluted mixture of HCOOH in He (1%) into the reactor. The sensitivity to $(HCO)_2$ at *m*/*e* 59 ($(HCO)_2 \cdot H^+$ ion) was assumed to be similar to the sensitivity to CH_2O at *m*/*e* 31 ($CH_2O \cdot H^+$ ion). This assumption is based on close values of the PTR rate constants for many organic molecules. For example, rate constants for $H_3O^+ + M \rightarrow MH^+ + H_2O$ reactions are (in 10^{-9} cm^3 molecule^{-1} s^{-1} units) (3.4 ± 0.9) for CH_2O, (3.6 ± 0.9) for CH_3CHO, (2.7 ± 0.8) for HCOOH, (3.0 ± 0.9) for CH_3COOH, and (2.8 ± 0.7) for CH_3OH.[15] The similar rates of these processes were confirmed in the present study by close values of the corresponding PTR detection sensitivities (in 10^8 molecule cm^{-3}/cps) for CH_2O (1.31 at *m*/*e* 31), $HOCH_2CHO$ (1.28 at *m*/*e* 61), HCOOH (1.22 at *m*/*e* 47), and CH_3OH (0.94 at *m*/*e* 33). Additional uncertainty of 20% was assigned to the measured concentration of glyoxal because of this assumption. The results of the measurements are presented in Table 2. Stability of GLAL concentration during the cooling of the gas mixture in the reactor was controlled by its mass-spectral peaks at *m*/*e* 61 and 79. Table 2 shows that the major product at 296 K is CH_2O with a yield of about 80%. However, its yield decreases to 50% when temperature decreases to 233 K. Similarly, the yield of $(HCO)_2$ drops from 14 to 4%. Conversely, the yield of HCOOH increases from about 18% to 52% in this temperature range.

CO_2. The yield of CO_2 was measured at 296 K with the H + NO_2 reaction as a source of OH radicals. The signal at *m*/*e* 60 (CO_3^- ion) overlapped with a minor peak of GLAL that largely lowered the signal-to-noise ratio. The CO_2 yield was determined both with respect to the consumed GLAL as $\Delta[CO_2]/\Delta[GLAL]$ and with respect to the OH consumed in the reaction with GLAL as $\Delta[CO_2]/\Delta[OH]_r$. In the latter case, the kinetics of OH decay was measured in the absence and in the presence of GLAL, and $\Delta[OH]_r$ was calculated as

$$\Delta[OH]_r = ([OH]_0 - [OH]_f) \cdot (k_{tot} - k_{loss}) / \{k_{tot} \cdot (1 - \Phi(OH))\}$$

where $[OH]_0$ and $[OH]_f$ are the initial and final OH concentration, respectively; k_{loss} and $k_{tot} = k_1 \cdot [GLAL] + k_{loss}$ are the first-order OH decay rate constants in the absence and presence of GLAL, respectively; and the coefficient $(1 - \Phi(OH))$ accounts for OH reformation at 296 K. Rate constants were determined from kinetic measurements as the slopes of the ln([OH]) versus reaction time plots (see, e.g., Figure 5a). Table 3 reports the results of four experiments giving an average CO_2 yield of (0.34 ± 0.04), where the uncertainty is 1σ for seven measured values.

HO_2. The yield of HO_2 was determined from kinetic measurements of OH and HO_2 concentrations in the OH + GLAL + O_2 system in the presence and absence of GLAL. Figure 6 gives an example of the kinetic curves of OH (solid symbols) and HO_2 (open symbols). The concentrations in this experiment were [GLAL] = 3.6×10^{12}, [O_2] = 2.1×10^{15}, and $[OH]_0 = 1.8 \times 10^{11}$ molecule cm^{-3}, using F + H_2O reaction to produce OH radicals. Formation of HO_2 in the absence of the reactant results from the dissociation of H_2O impurity in the discharge producing H-atoms which recombine with O_2 in the TFR. $\Delta[HO_2]$ was calculated as a difference between the HO_2 concentrations with and without the reactant, because GLAL cannot compete with O_2 for H-atom reaction under the conditions of our experiments. The loss of OH and HO_2 in the absence of GLAL corresponded to the first-order rate constants 26 s^{-1} and 14 s^{-1}, respectively, and occurred through the OH + HO_2 reaction and wall decay. The HO_2 yield was determined at $t \approx 10$ ms when HO_2 background concentration was close to its maximum and the error in $\Delta[HO_2]$ because of loss was about 10% as estimated by simulation calculations. HO_2 signal was calibrated using the HO_2 + NO reaction as described in ref 14. $\Delta[OH]_r$ was calculated from the OH kinetics as in the previous paragraph. The data from this experiment (Figure 6) are given in the upper row of Table 4. Table 4 also reports results of other similar experiments carried out with different GLAL and initial OH concentrations. The average HO_2 yield is (0.77 ± 0.09), where the uncertainty is 1σ for four measured values. Taking into account the errors due to HO_2 loss and uncertainties in calibration, the final result can be given as $\Phi(HO_2) = (0.77 \pm 0.12)$.

A summary of the product yields in the OH + GLAL + O_2 chemical system is presented in Table 5. The yields were determined in excess of GLAL over OH at O_2 concentrations sufficiently high for completion of reactions of the intermediate products with O_2. The quoted uncertainties include statistical deviations of the measured signals and systematic errors of calibration. The obtained temperature dependence of the yields is similar to that in the OH + hydroxyacetone + O_2 system:[12] the yields of aldehydes decrease and the yield of acid increases with the decrease of temperature. We suggest below a mechanism which can explain formation of formic acid, partial reformation of OH, and temperature behavior of the yields.

3.3. Mechanism of the OH-Initiated Oxidation of Glycolaldehyde. The product formation observed can be explained by reactions of the primary radicals from reaction (1) with oxygen. These reactions should be fast enough to generate the "final" products within reaction times less than 30 ms under our

TABLE 2: Measurements of the Yields of Formaldehyde, Φ(CH_2O), Glyoxal, Φ($(HCO)_2$), and Formic Acid, Φ(HCOOH), in PTR Regime[a]

T (K)	Δ[GLAL]	Δ[CH_2O]	Δ[$(HCO)_2$]	Δ[HCOOH]	Φ(CH_2O)	Φ($(HCO)_2$)	Φ(HCOOH)
296	1.93	1.63	0.285	0.357	0.82	0.14	0.18
	1.84	1.62	0.301	0.391	0.77	0.14	0.19
273	1.95	1.43	0.259	0.445	0.72	0.13	0.23
253	2.10	1.40	0.143	0.540	0.71	0.072	0.27
	2.05	1.25	0.188	0.612	0.67	0.093	0.30
245	2.06	1.34	0.119	0.758	0.62	0.060	0.38
239	1.89	1.09	0.080	0.811	0.55	0.040	0.41
233	2.05	0.99	0.083	1.04	0.50	0.041	0.52

[a] Concentrations are in 10^{11} molecule cm^{-3}; Δ[M] denotes a change of concentration at $t = 27$ ms with switching the discharge on.

TABLE 3: Measurement of the CO_2 Yield at 296 K[a]

[GLAL]	[O_2]	k_{loss}	k_{tot}	$[OH]_0$	$\Delta[OH]_r$	Δ[GLAL]	Δ[CO_2]	Φ(CO_2)[b]	Φ(CO_2)[c]
33	2.5×10^4	28.5	48.9	3.79	1.10	1.28	0.38	0.35	0.30
33	1.4×10^4	28.5	48.9	3.79	1.04	1.17	0.39	0.37	0.33
176	1.2×10^4					8.11	2.76		0.34
47	1.2×10^4	22.0	52.5	5.50	2.32	1.72	0.71	0.31	0.41

[a] Concentrations are in 10^{11} molecule cm^{-3}. [b] $\Phi(CO_2) = \Delta[CO_2]/\Delta[OH]_r$. [c] $\Phi(CO_2) = \Delta[CO_2]/\Delta[GLAL]$.

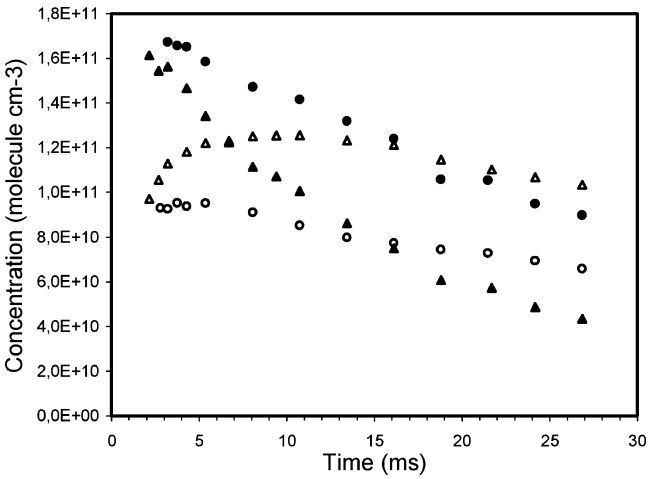

Figure 6. Temporal profiles of OH (solid symbols) and HO_2 (open symbols) concentrations in the absence of GLAL (circles) and presence of GLAL (triangles).

experimental conditions. By final products, we mean stable molecules and HO_2 radical which lifetime exceeds the residence time in the TFR. Let us denote **A** and **B** the radicals formed in reaction (1a) and (1b), respectively:

$$OH + HOCH_2CHO \rightarrow HOCH_2CO\ (\mathbf{A}) + H_2O \quad (1a)$$

$$OH + HOCH_2CHO \rightarrow HOCHCHO\ (\mathbf{B}) + H_2O \quad (1b)$$

Fate of Radical A. Radical **A** can decompose to CH_2OH and CO or react with oxygen. Decomposition path (reaction (15)) will be followed by reaction with oxygen (reaction (5)) producing formaldehyde and HO_2:

$$HOCH_2CO \rightarrow CH_2OH + CO \quad (15)$$

$$CH_2OH + O_2 \rightarrow CH_2O + HO_2 \quad (5)$$

The decomposition rate of $HOCH_2CO$ was calculated to be $k_{15} = 3 \times 10^4\ s^{-1}$ at 1 atm and 298 K using G2/RRKM approach.[17] Assuming a linear dependence of k_{15} on pressure in this range, we obtain for our conditions a value of about $1 \times 10^4\ s^{-1}$, corresponding to a characteristic decomposition time of 0.1 ms. It means, that assuming a typical rate constant of reaction with oxygen $k(\mathbf{A} + O_2) = 4 \times 10^{-12}$ cm^3 $molecule^{-1}$ s^{-1}, decomposition should be faster if oxygen concentration is less than 3×10^{15} molecule cm^{-3}. Rate constant of reaction (5) is $k_5 = 9.6 \times 10^{-12}$ cm^3 $molecule^{-1}$ s^{-1},[18] which should result in a rapid formation of formaldehyde even at the low background oxygen concentration. However, we present below evidence that the rate of CH_2O formation is not so fast as expected from reactions (15) and (5). If the decomposition is slower than predicted by Méreau et al.,[17] other mechanisms involving the reaction of radical **A** with O_2 are possible. In any case, reaction of **A** with O_2 will be more likely than decomposition under atmospheric conditions. The radical **A** has two conformers corresponding to trans ($\mathbf{A_1}$) and cis ($\mathbf{A_2}$) orientation of the hydroxyl group with respect to carbonyl O-atom (see scheme below). These two conformers have been found theoretically by Galano et al.[19] as the products of the abstraction of the aldehydic H-atom from the two (cis and trans) conformations of the initial GLAL molecule. The calculation at CCSD(T)//B&HLYP/6-311++G(d,p) level gave an energy for the trans-conformer ($\mathbf{A_1}$) 2.0 kcal mol^{-1} lower than for the cis-one ($\mathbf{A_2}$). Formation of hydrogen bond in each of these conformers with approaching oxygen molecule can lead to the abstraction of the end hydrogen atom followed by decomposition of OCH_2CO to CH_2O and CO (channel 2a):

$$O_2 + HOCH_2CO \rightarrow HO_2 + CH_2O + CO \quad (2a)$$

Reaction (2a) is indistinguishable from the sequence of reactions (15−5) since they give the same products. However, measurements of the rate of CH_2O formation at increasing O_2 concentrations favor reaction (2a) (see last paragraph). Another possibility is addition of oxygen forming the $\mathbf{A}-O_2$ peroxy adduct. Peroxy radical concentration about a few 10^{11} molecule cm^{-3} is too low to explain production of the final products from the reactions between peroxy radicals. Our results show that the peroxy adducts, if formed, would rapidly decompose to final products in two different ways (channels 2b and 2c):

$$HOCH_2CO + O_2 \rightarrow HOCH_2C(O)OO \rightarrow CO_2 + CH_2O + OH \quad (2b)$$

$$HOCH_2CO + O_2 \rightarrow HOCH_2C(O)OO \rightarrow CO_2 + HCOOH + H \quad (2c)$$

Adduct $\mathbf{A_1}-O_2$ can decompose through a six-centered transition state to produce CO_2, formaldehyde, and OH, whereas adduct

TABLE 4: Measurement of the HO_2 Yield at 296 K[a]

[GLAL]	$[O_2]$	k_{loss}	k_{tot}	$[OH]_0$	t (ms)	Δ[OH]	$\Delta[OH]_r$	$\Delta[HO_2]$	$\Phi(HO_2)$
36	2.1×10^4	26.0	54.8	1.82	10.7	0.538	0.456	0.403	0.88
92	2.3×10^4	34.7	122.7	2.02	10.5	1.55	1.48	0.960	0.65
136	1.8×10^3	24.8	136.4	1.12	15.8	1.03	0.843	0.723	0.71
24	1.6×10^4	25.0	39.5	3.82	7.0	1.08	0.528	0.438	0.83

[a] Concentrations are in 10^{11} molecule cm^{-3}; first-order rate constants are in s^{-1}.

TABLE 5: Summary of the Product Yields (in %) in the OH + Glycolaldehyde + O_2 Chemical System

T (K)	CH_2O	$(HCO)_2$	HCOOH	CO_2	HO_2	OH
296	80 ± 7	14 ± 4	18 ± 6	34 ± 7	77 ± 12	25 ± 3
273	72 ± 7	13 ± 3	23 ± 8			33 ± 4
253	69 ± 8	8 ± 2	29 ± 8			36 ± 4
233	50 ± 7	4 ± 1	52 ± 12			44 ± 5

$\mathbf{A_2}-O_2$ can yield CO_2, formic acid, and H-atom via a four-centered transition state as illustrated by the following scheme:

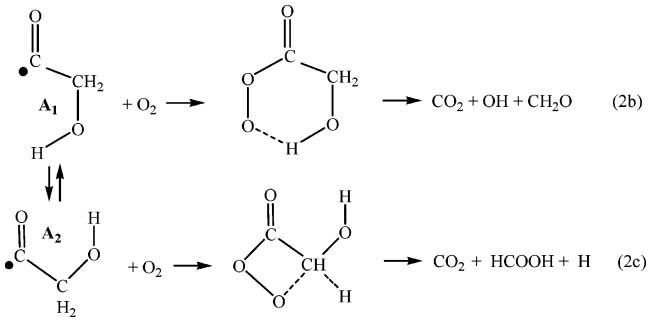

*Fate of Radical **B***. Similarly, abstraction of hydrogen atom from the hydroxyl group of radical **B** results in glyoxal (channel 6a), and addition of oxygen to radical **B** followed by C−C bond rupture can produce formic acid (channel 6b):

$$HOCHCHO + O_2 \rightarrow (HCO)_2 + HO_2 \qquad (6a)$$

$$HOCHCHO + O_2 \rightarrow HC(O)CH(OH)OO \rightarrow CO + HCOOH + OH \qquad (6b)$$

Reaction (6b) can proceed via a five-membered transition state:

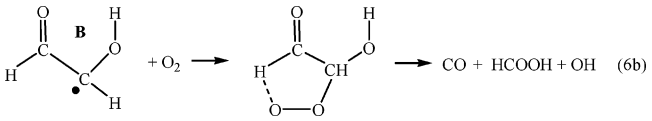

Branching Ratios. Branching ratios for reactions (1), (2), and (6) at 296 K can be calculated from the measured product yields. The sum of the CH_2O, $(HCO)_2$, and HCOOH yields, (112 ± 11)%, encompasses unity taking into account the experimental errors. These yields were normalized to 100%, becoming 71%, 13%, and 16%, respectively. Then, simple calculation with account of the yield of CO_2 and OH reformation gives the branching ratio (2a):(2b):(2c):(6a):(6b) = 49:22:13:13:3. From this ratio, the yield of HO_2, produced in reactions (2a), (2c), and (6a), should be 75% which well agrees with the average measured value of 77%. This ratio corresponds to $k_{1a}:k_{1b} = 84:16$ for initiation reaction in agreement with the results of Niki et al.[1] and Magneron et al.[10] The branching ratios for reactions (2) and (3) are $k_{2a}:k_{2b}:k_{2c} = 58:26:15$ and $k_{6a}:k_{6b} = 81:19$.

If reactions (2) and (6) have lower barriers for the HOOH-forming transition states than those for reactions (2a) and (6a), a decrease of temperature will lead to a growing contribution of channels (2b), (2c), and (6b) and, hence, to the increase of the formic acid yield and to the decrease of the formaldehyde and glyoxal yields. This tentative mechanism needs theoretical verification, that is, calculation of the potential energy surfaces for the reactions of the radicals **A** and **B** with O_2.

Kinetics of CH_2O and $(HCO)_2$ Product Formation. The measurement of CH_2O formation time profiles at different O_2 concentrations was undertaken to determine the fate of the primary $HOCH_2CO$ radical (decomposition versus reaction with O_2). The measurements at *m*/*e* 31 and 49 gave identical results which are presented in Figure 7a. Simultaneously, the $(HCO)_2$ signal at *m*/*e* 59 was recorded to evaluate the rate constant of reaction (6) (Figure 7b). The concentrations in the reactor during this experiment were $[GLAL] = 7.2 \times 10^{12}$ and $[OH]_0 = 4.9 \times 10^{11}$ molecule cm^{-3}. Oxygen concentration was varied from 1.5×10^{13} to 1.7×10^{14} molecule cm^{-3}; at higher concentrations, CH_2O and $(HCO)_2$ signals were practically insensitive to $[O_2]$. The best fit between experimental and simulated (solid curves)

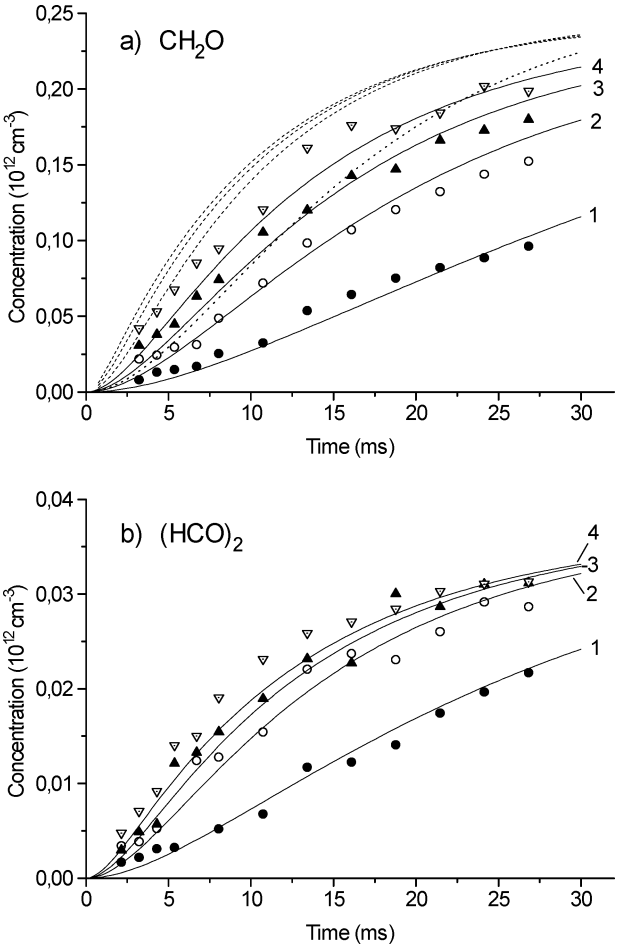

Figure 7. Temporal profiles of CH_2O (a) and $(HCO)_2$ (b) formation at different O_2 concentrations: $[O_2] = 1.5 \times 10^{12}$ (•), 6.1×10^{13} (○), 1.0×10^{14} (▲), and 1.7×10^{14} (▽) molecule cm^{-3}. Solid curves are simulated ones with $k_2 = 2 \times 10^{-12}$ and $k_6 = 3.5 \times 10^{-12}$ cm^3 $molecule^{-1}$ s^{-1}. Dotted and dashed curves correspond to curve 1 and curves 2−4 when reaction (2) is substituted by reactions (15) and (5).

concentration−time profiles of CH_2O and $(HCO)_2$ was obtained for the rate constants $k(CH_2O) = 1.7 \times 10^{-12}$ and $k((HCO)_2) = 2.8 \times 10^{-12}$ cm^3 molecule^{-1} s^{-1} for CH_2O formation in reaction (2) and $(HCO)_2$ formation in reaction (6), respectively. These rate constants correspond to $k_{2a} + k_{2b}$ and k_{6a}, respectively, and, taking into account the branching ratios for reactions (2) and (6), we obtain the following estimated values: $k_2 \approx 2 \times 10^{-12}$ and $k_6 \approx 3.5 \times 10^{-12}$ cm^3 molecule^{-1} s^{-1}. The dotted curve in Figure 7a was calculated for the lowest concentration $[O_2] = 1.5 \times 10^{12}$ molecule cm^{-3}, assuming a rapid decomposition of $HOCH_2CO$ radical followed by reaction (5). Dashed curves correspond to curves 2−4 when reaction (2) is substituted by reactions (15) and (5). This mechanism would lead to a full transformation to CH_2O even at background O_2 levels, which is evidently not the case. This suggests that the decomposition of the $HOCH_2CO$ radical is not so fast as theoretically predicted.[17] The rate constant of reaction (6a), $k_{6a} \approx 3 \times 10^{-12}$ cm^3 molecule^{-1} s^{-1}, is noticeably lower than those for analogous O_2 reactions forming aldehydes: $CH_2OH + O_2$ ($k_5 = 9.6 \times 10^{-12}$ cm^3 molecule^{-1} s^{-1}) or $CH_3CHOH + O_2$ ($k = 1.9 \times 10^{-11}$ cm^3 molecule^{-1} s^{-1}). This can be explained by the fact that the radical **B** is a vinoxy-resonance stabilized radical having a part of electron population on the oxygen, which hinders interaction with O_2.

4. Atmospheric Implication

Up to now, in the chemical mechanisms of atmospheric models, it was supposed that only CH_2O, $(HCO)_2$, and HO_2 were produced in the degradation of GLAL.[4,7,20] In this respect, the main result of the present study is that oxidation of GLAL yields formic acid along with the aldehydic products. The production of the acid is especially important at the low temperatures of the upper troposphere (UT). This change in product distribution at low temperature will reduce the role of GLAL as a net source of HO_x in the UT. Effectively, the carbonyl species CH_2O and $(HCO)_2$, considered so far as the products of the OH-initiated oxidation of GLAL, are net sources of HO_x through OH reaction or photolysis. Conversely, HCOOH is relatively stable with respect to both OH reaction and photolysis, and it is mostly washed out from the atmosphere (the typical lifetimes of CH_2O and $(HCO)_2$ in the UT are a few hours and that of HCOOH is more than 1 month). This reduction of the HO_x formation potential of GLAL will also reduce the HO_x formation potential of its precursors, such as isoprene,[7,8] which is transported from the surface to the UT by fast convection and is further oxidized in the UT to produce GLAL among other products.

Acknowledgment. The work was carried out within the UTOPIHAN-ACT and SCOUT projects of the European Union and the National Programme of Atmospheric Chemistry (PNCA) of CNRS.

References and Notes

(1) Niki, H.; Maker, P. D.; Savage, C. M.; Hurley, M. D. *J. Phys. Chem.* **1987**, *91*, 2174.
(2) Orlando, J. J.; Tyndall, G. S.; Bilde, M.; Ferronato, C.; Wallington, T. J.; Vereecken, L.; Peeters, J. *J. Phys. Chem. A* **1998**, *102*, 8116.
(3) Ferronato, C.; Orlando, J.J.; Tyndall, G. S. *J. Geophys. Res.* **1998**, *103* (D19), 25579.
(4) Carter, W. P. L.; Atkinson, R. *Int. J. Chem. Kinet.* **1996**, *28*, 497.
(5) Mason, S. A.; Field, R. J.; Yokelson, R. J.; Kochivar, M. A.; Tinsley, M. R.; Ward, D. E.; Hao, W. M. *J. Geophys. Res.* **2001**, *106*, 12527.
(6) Grossmann, D.; Moortgat, G. K.; Kibler, M.; Schlomski, S.; Bächmann, K.; Alicke, B.; Geyer, A.; Platt, U.; Hammer, M.-U.; Vogel, B.; Mihelcic, D.; Hofzumahaus, A.; Holland, F.; Volz-Thomas, A. *J. Geophys. Res.* **2003**, *108* (D4), 8250.
(7) von Kuhlmann, R.; Lawrence, M. G.; Pöschl, U.; Crutzen, P. *J. Atmos. Chem. Phys.* **2004**, *4*, 1.
(8) Doherty, R. M.; Stevenson, D. S.; Collins, W. J.; Sanderson, M. G. *Atmos. Chem. Phys. Discuss.* **2005**, *5*, 3747.
(9) Bacher, C.; Tyndall, G. S.; Orlando, J. J. *J. Atmos. Chem.* **2001**, *39*, 171.
(10) Magneron, I.; Mellouki, A.; Le Bras, G.; Moortgat, G. K.; Horowitz, A. Wirtz, K. *J. Phys. Chem. A* **2005**, *109*, 4552.
(11) Karunanandan, R.; Hölscher, D.; Dillon, T. J.; Horowitz, A.; Crowley, J. N. *J. Phys. Chem. A* **2006**, submitted.
(12) Butkovskaya, N. I.; Pouvesle, N.; Kukui, A.; Mu, Yu.; Le Bras, G. *J. Phys. Chem. A* **2006**, *110*, 6833.
(13) Kukui, A.; Borissenko, D.; Laverdet, G.; Le Bras, G. *J. Phys. Chem. A* **2003**, *107*, 5732.
(14) Butkovskaya, N. I.; Kukui A.; Pouvesle, N.; Le Bras, G. *J. Phys. Chem. A* **2005**, *109*, 6509.
(15) Ikezoe, Y.; Matsuoka, S.; Takebe, M.; Viggiano, A. *Gas Phase Ion-Molecule Reaction Rate Constants through 1986*; Ion Reaction Research Group of the Mass Spectrometry Society of Japan, Maruzen Company: Tokyo, 1987.
(16) Elrod, M. J.; Ranschaert, D. L.; Schneider, N. J. *Int. J. Chem. Kinet.* **2001**, *33*, 363.
(17) Méreau, R.; Rayez, M.-T.; Rayez, J.-C.; Caralp, F.; Lesclaux, R. *Phys. Chem. Chem. Phys.* **2001**, *3*, 4712.
(18) NIST Chemical Kinetics Database, Standard Reference Database 17, Web Version 7.0, Release 1.3, NIST, Gaithersburg, MD.
(19) Galano, A.; Alvarez-Idaboy, J. R.; Ruiz-Santoyo, M. E.; Vivier-Bunge, A. *J. Phys. Chem. A* **2005**, *109*, 169.
(20) Pöschl, U.; von Kuhlmann, R.; Poisson, N.; Crutzen, P. *J. Atmos. Chem.* **2000**, *37*, 29.